© Pol J Radiol 2025; 90 : e103-e113
DOI: https://doi.org/10.5114/pjr/200967

Received: 05.02.2025
Accepted: 07.02.2025
Published: 20.02.2025

Polish Journal of Radiology

http://www.polradiol.com

Original paper

Diffusion imaging in gliomas: how ADC values forecast glioma genetics

Paulina Śledzińska-Bebyn[1,A,B,C,D,E,F], Jacek Furtak[2,3,D,G], Marek Bebyn[4,C,E], Alicja Bartoszewska-Kubiak[5,B], Zbigniew Serafin[6,A,D,G]

[1]Department of Radiology, 10th Military Research Hospital and Polyclinic, Bydgoszcz, Poland
[2]Department of Clinical Medicine, Faculty of Medicine, University of Science and Technology, Bydgoszcz, Poland
[3]Department of Neurosurgery, 10th Military Research Hospital and Polyclinic, Bydgoszcz, Poland
[4]Department of Internal Diseases, 10th Military Clinical Hospital and Polyclinic, Bydgoszcz, Poland
[5]Laboratory of Clinical Genetics and Molecular Pathology, Department of Medical Analytics, 10th Military Research Hospital and Polyclinic, Bydgoszcz, Poland
[6]Faculty of Medicine, Bydgoszcz University of Science and Technology, Bydgoszcz, Poland

Abstract

Purpose: This study investigates the relationship between diffusion-weighted imaging (DWI) and mean apparent diffusion coefficient (ADC) values in predicting the genetic and molecular features of gliomas. The goal is to enhance non-invasive diagnostic methods and support personalised treatment strategies by clarifying the association between imaging biomarkers and tumour genotypes.

Material and methods: A total of 91 glioma patients treated between August 2023 and March 2024 were included in the analysis. All patients underwent preoperative magnetic resonance imaging (MRI), including DWI, and had available histopathological and genetic test results. Clinical data, tumour characteristics, and genetic markers such as *IDH1* mutation, *MGMT* promoter methylation, *EGFR* amplification, *TERT* pathogenic variant, and *CDKN2A* deletion were collected. Statistical analysis was performed to identify correlations between ADC values, MRI perfusion parameters, and genetic characteristics.

Results: Significant associations were found between lower ADC values and aggressive tumour features, including *IDH1*-wildtype, *MGMT* unmethylated status, *TERT* pathogenic variant, and *EGFR* amplification. Additionally, distinct ADC patterns were observed in gliomas with *CDKN2A*, *TP53*, and *PTEN* gene deletions. These findings were further supported by contrast enhancement and other MRI parameters, indicating their role in tumour characterisation.

Conclusions: DWI and ADC measurements demonstrate strong potential as non-invasive tools for predicting glioma genetics. These imaging biomarkers can aid in tumour characterisation and provide valuable insights for guiding personalised treatment strategies.

Key words: diffusion-weighted imaging, apparent diffusion coefficient, glioma, MRI, tumour characterisation.

Introduction

Gliomas are a diverse group of primary brain tumours distinguished by their different clinical behaviour, histological characteristics, and genetic profiles. Therefore, it is crucial to make precise evaluations and descriptions of these tumours for precise diagnoses to optimise treatment approaches and enhance patient results [1]. Obtaining histopathological specimens for accurate diagnosis might be challenging in clinical situations in which surgery is not possible. To overcome these challenges, it is essential to utilise non-invasive diagnostic technologies to improve the effectiveness and precision of diagnosis.

Correspondence address:
Paulina Śledzińska-Bebyn, Department of Radiology, 10th Military Research Hospital and Polyclinic, 5 Powstańców Warszawy St., 85-681 Bydgoszcz, Poland, e-mail: paula.sledzinska@gmail.com

Authors' contribution:
A Study design · **B** Data collection · **C** Statistical analysis · **D** Data interpretation · **E** Manuscript preparation · **F** Literature search · **G** Funds collection

Although traditional imaging modalities are beneficial, they often lack the information required for a full examination of tumours. This gap has generated curiosity in more sophisticated imaging methods, including diffusion-weighted imaging (DWI) and its derivative – the apparent diffusion coefficient (ADC).

DWI utilises the motion of water molecules in tissue to generate contrast in magnetic resonance images (MRI). The ADC values obtained by DWI yield quantitative assessments of water diffusion, which are inversely correlated with cellular density and the integrity of cellular structures. When studying gliomas, it has been observed that ADC levels are related to the density of tumour cells, their growth rate, and the presence of dead tissue. This method offers a more indirect way of determining the histological and genetic characteristics of the tumour, eliminating the necessity for invasive procedures [2].

Recent research has shown that ADC measures can be used to differentiate between low-grade and high-grade gliomas and to predict certain genetic alterations, such as isocitrate dehydrogenase (*IDH*) status [3,4]. These insights are vital because genetic alterations in glioma have a considerable impact on prognosis and therapy response. For example, gliomas with *IDH* mutations typically correspond to more favourable outcomes and have different metabolic pathways compared to gliomas without *IDH* alterations [5]. Furthermore, evaluating the status of the *IDH1* gene is the initial stage in determining the accurate genetic profile of glioma, serving as an indicator for subsequent genetic analyses [6].

The present study aims to explore the relevance of diffusion imaging, specifically ADC values, in predicting glioma genetics and tumour features. Through the synthesis of current research and clinical data, we seek to clarify how modern imaging techniques might improve our understanding of glioma biology and aid in the development of individualised treatment strategies.

Material and methods

Patient cohort

The research study contains a cohort of 91 individuals who received neurosurgical treatment between August 2023 and March 2024. The inclusion criteria encompassed individuals aged 18 years and above who received preoperative MRI with DWI assessment and had accessible histopathological and genetic test findings. Patients who had incomplete datasets were not included in the study. The study obtained approval from the institutional Bioethics Committee.

Clinical data collection

The clinical data obtained encompassed demographic information, such as age and sex, along with tumour features, including location, laterality, and multiplicity. The recorded additional information included clinical symptoms, history of recurrence, Karnofsky performance status (KPS), handedness, smoking status, particular tumour diagnosis, tumour grade, and body mass index (BMI).

MRI protocol

MRI examinations were conducted using a 1.5 T MRI scanner, using a standardised protocol (Supplementary Table 1) to maintain consistency and reproducibility of imaging data. The sequences comprised pre- and post-gadolinium T1- and T2-weighted images, fluid-attenuated inversion recovery (FLAIR), DWI, and dynamic susceptibility contrast (DSC) imaging. Post-contrast images were acquired after administering a bolus injection of a gadolinium-based contrast agent at a dose of 0.1 mmol/kg body weight, followed by a saline flush.

Radiological variables

The images were examined on the analysis software Philips Intellispace Portal. The radiological characteristics assessed included components from the Vasari classification [7]. The features encompassed multifocal lesions, contrast enhancement characteristics, T2/FLAIR mismatch, intratumoural necrosis, maximal diameter, tumour volume, involvement of the corpus callosum, involvement of the cortex, extension into the ependymal layer, and invasion of the pia mater. In addition, ADC was measured in DWI, while relative cerebral blood volume (rCBV) and relative cerebral blood flow (rCBF) were analysed using DSC imaging the average. The regions of interest (ROIs) were positioned according to the method previously outlined by Xing *et al.* [4]. To accurately position the ROIs on the solid tumour components and avoid areas with cysts, bleeding, necrosis, or swelling around the tumour, the DWI pictures were aligned with conventional MRI scans, including T1-weighted scans before and after the injection of gadolinium and T2-weighted scans. Therefore, the average ADC values were determined by manually positioning between 3 and 5 non-overlapping ROIs positioned within the tumour regions of the visually lowest ADC values.

Histopathological and genetic analysis

The histopathological diagnosis was determined by the most recent WHO CNS5 classification [8]. The genetic indicators that were evaluated were *IDH1* mutation status, O^6-methylguanine-DNA methyltransferase (*MGMT)* methylation, epidermal growth factor receptor (*EGFR)* amplification, cyclin-dependent kinase inhibitor 2A (*CDKN2A)* deletion, *TP53* deletion, platelet-derived growth factor receptor alpha gene (*PDGFRA)* amplification, phosphatase and tensin homologue (*PTEN)* deletion, 1p/19q codeletion, telomerase reverse transcriptase (*TERT)* patho-

genic variants, and *H3F3A* (K27M) pathogenic variants. The markers were chosen based on their well-established significance in brain tumour pathophysiology and prognosis. Standard molecular techniques, such as polymerase chain reaction (PCR), fluorescence in situ hybridisation (FISH), and next-generation sequencing (NGS), were employed for genetic analysis.

Statistical analysis

The normality of the data was evaluated using the Shapiro-Wilk test. The selection of statistical tests, either the Mann-Whitney *U* test or the χ^2 test, depended on whether the data were continuous or categorical. These tests were used to identify any significant differences between the 2 groups of independent variables. Instances with incomplete genetic data were omitted from the statistical analysis to ensure uniformity. The results were presented using 95% confidence intervals (95% CI), and statistical significance was determined by a *p*-value of less than 0.05. The statistical studies were performed using R Studio software.

Results

Demographic and clinical characteristics

Table 1 provides a comprehensive summary of the demographic and clinical characteristics of the 91 patients included in this study.

The cohort comprised a slightly higher proportion of males (52.7%) than females (47.3%), with a mean age of 52 years (SD = 15 years). The malignancies were predominantly found in the temporal (35.2%) and frontal lobes (34.1%). The tumours were evenly distributed across the left and right hemispheres, with each hemisphere accounting for 46.2% of the cases. A minor fraction of tumours (7.7%) affected both hemispheres simultaneously.

The prevalent clinical symptoms were headache (27.5%), epilepsy (26.4%), and paresis (24.2%). Additional symptoms that were documented included speech difficulties (19.8%), vision disturbances (15.4%), memory disorders (11%), ataxia (9.9%), dizziness (4.4%), and paraesthesia (5.5%). A significant proportion of patients, specifically 9.9%, exhibited no symptoms.

The patients' KPS had a mean value of 81 (SD = 12), suggesting that most patients had a relatively high level of functional ability during the examination.

Table 2 provides a comprehensive overview of the diagnosis and molecular characteristics of the study participants.

Among the 91 patients included in the study, 29.7% were diagnosed with astrocytoma, and 70.3% with glioblastoma. The tumours were graded according to the WHO classification, with 9 patients (9.9%) having grade 2 tumours, 17 patients (18.7%) having grade 3 tumours, and 65 patients (71.4%) having grade 4 tumours.

Table 1. Patients' characteristics

Factor	*n*	%
Sex		
Female	43	47.3
Male	48	52.7
Age (Mean; SD)	52	15
Handedness		
Left	2	2.2
Right	72	79.1
Both	2	2.2
NA	15	16.5
Location		
Temporal lobe	32	35.2
Frontal lobe	31	34.1
Parietal lobe	15	16.5
Occipital lobe	4	4.4
Cerebellum	3	3.3
Corpus callosum	3	3.3
Brainstem	2	2.2
Insular	1	1.1
Side		
Left	42	46.2
Right	42	46.2
Both	7	7.7
Paresis	22	24.2
Paraesthesia	5	5.5
Speech disorders	18	19.8
Headache	25	27.5
Dizziness	4	4.4
Epilepsy	24	26.4
Ataxia	9	9.9
Vision disturbance	14	15.4
Memory disorders	10	11
No symptoms	9	9.9
Recurrence	29	31.9
KPS (mean; SD)	81	12
Nicotinism		
No	54	59.3
Yes	11	12.1
NA	26	48.6
BMI (mean; SD)	26.14	4.7

SD – standard deviation, KPS – Karnofsky Performance Scale

The analysis of *IDH1* mutation status revealed that 71.4% of patients had *IDH1*-wildtype tumour, while 28.6% of patients had *IDH1* mutations. Regarding *MGMT*

Table 2. Diagnosis and molecular characteristics

	n	%
Diagnosis		
Astrocytoma	27	29.7
Glioblastoma	64	70.3
Grade		
2	9	9.9
3	17	18.7
4	65	71.4
IDH1 mutation		
Wildtype	65	71.4
Mutant	26	28.6
MGMT methylation		
Unmethylated	33	37.9
Methylated	54	62.1
EGFR amplification		
No	40	46.0
Yes	47	54.0
CDKN2A deletion		
Non-deleted	41	45.1
Heterozygous deletion	28	30.8
Homozygous deletion	17	18.7
NA	5	5.5
TP53 deletion		
Non-deleted	78	85.7
Deleted	3	3.3
NA	10	11.0
PDGFRA amplification		
Non-amplified	67	73.6
Amplified	14	15.4
NA	10	11.0
PTEN deletion		
Non-deleted	45	49.5
Deleted	35	38.5
NA	11	12.1
1p19q codeletion		
Non-codeleted	86	98.9
Codeleted	1	1.1
TERT pathogenic variant		
No	34	37.4
Yes	44	48.4
NA	13	14.3
H3K27M pathogenic variant		
No	68	74.7
NA	23	25.3
Multifocal lesion		
No	68	74.7
Yes	23	25.3

IDH1 – isocitrate dehydrogenase 1, *MGMT* – O^6-methylguanine-DNA methyltransferase; *EGFR* – epidermal growth factor receptor, *CDKN2A* – loss of cyclin-dependent kinase inhibitor 2A, *PDGFRA* – platelet-derived growth factor receptor alpha gene, *PTEN* – phosphatase and tensin homologue, *TERT* – telomerase reverse transcriptase

promoter methylation, 37.9% of patients were found to have *MGMT* promoter unmethylated, whereas 62.1% of patients had *MGMT* promoter methylated. *EGFR* amplification was present in 54% of patients. *CDKN2A* deletion status indicated that 45.1% of patients had non-deleted *CDKN2A*, 30.8% of patients had heterozygous deletions, and 18.7% of patients had homozygous deletions. *TP53* deletion was found in 3.3% of patients. *PDGFRA* amplification was observed in 15.4% of patients. *PTEN* deletion was detected in 38.5% of patients. Only one patient had 1p/19q codeletion, while the vast majority (98.9%) did not have this genetic feature. *TERT* pathogenic variants were identified in 48.4% of patients. Representative patients' examinations are presented in Figures 1–3.

Table 3 outlines the imaging parameters assessed in the study.

Contrast enhancement was observed in 67 patients (73.6%), while 24 patients (26.4%) showed no enhancement. The quality of enhancement was graded as follows: 0 means no enhancement (26.4%), 1 means mild/minimal enhancement (13.2%), and 2 means marked/avid enhancement (62.6%). T2/FLAIR mismatch was present in 9 patients (9.9%). The mean rCBF was 4.1, and the mean rCBV was 5.2. Intratumoural necrosis was noted in 66 patients (72.5%). The maximal diameter of the tumours had a mean of 44.6 mm, and the mean tumour volume was 31.2 cm^3. The mean ADC was 1.36×10^{-3} mm^2/s. Corpus callosum involvement was observed in 25 patients (27.5%), while cortical involvement was noted in 77 patients (84.6%). Ependymal extension was present in 59 patients (64.8%), and pial invasion was seen in 68 patients (74.7%).

Table 4 provides a comprehensive analysis of the relationship between various MRI perfusion parameters and genetic features in gliomas.

Patients with *IDH1*-wildtype gliomas exhibited a significantly lower mean ADC value compared to those with *IDH1* mutations ($p < 0.05$). Contrast enhancement was significantly more frequent in *IDH1*-wildtype gliomas compared to *IDH1* mutant gliomas ($p < 0.05$). Enhancement quality, T2/FLAIR mismatch, and other variables also varied significantly between these 2 groups ($p < 0.05$).

Gliomas without *MGMT* promoter methylation had a significantly lower mean ADC value compared to *MGMT* promoter methylated gliomas ($p < 0.05$). Contrast enhancement was observed more frequently in gliomas

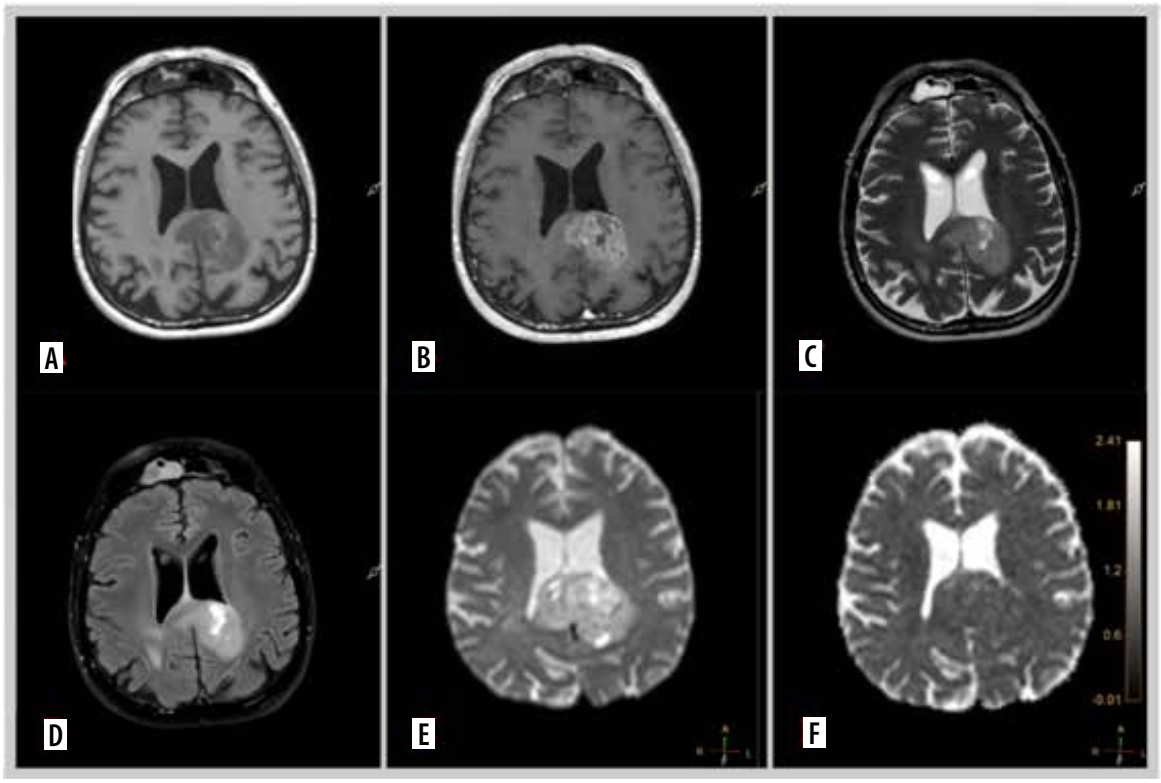

Figure 1. Representative magnetic resonance images of examined patient. A 68-year-old man with glioblastoma G4. Molecular characteristics: *IDH1*-wild-type, present *TERT* promoter pathogenic variant, *CDKN2A* homozygous deletion, *EGFR* amplification, *MGMT* promoter unmethylated. **A)** Pre-contrast T1. **B)** Contrast enhanced tumour on T1 post gadolinium. **C)** T2-weighted scan. **D)** Fluid-attenuated inversion recovery (FLAIR). **E**) Diffusion-weighted imaging (DWI). **F)** Reduced diffusion on apparent diffusion coefficient (ADC) map

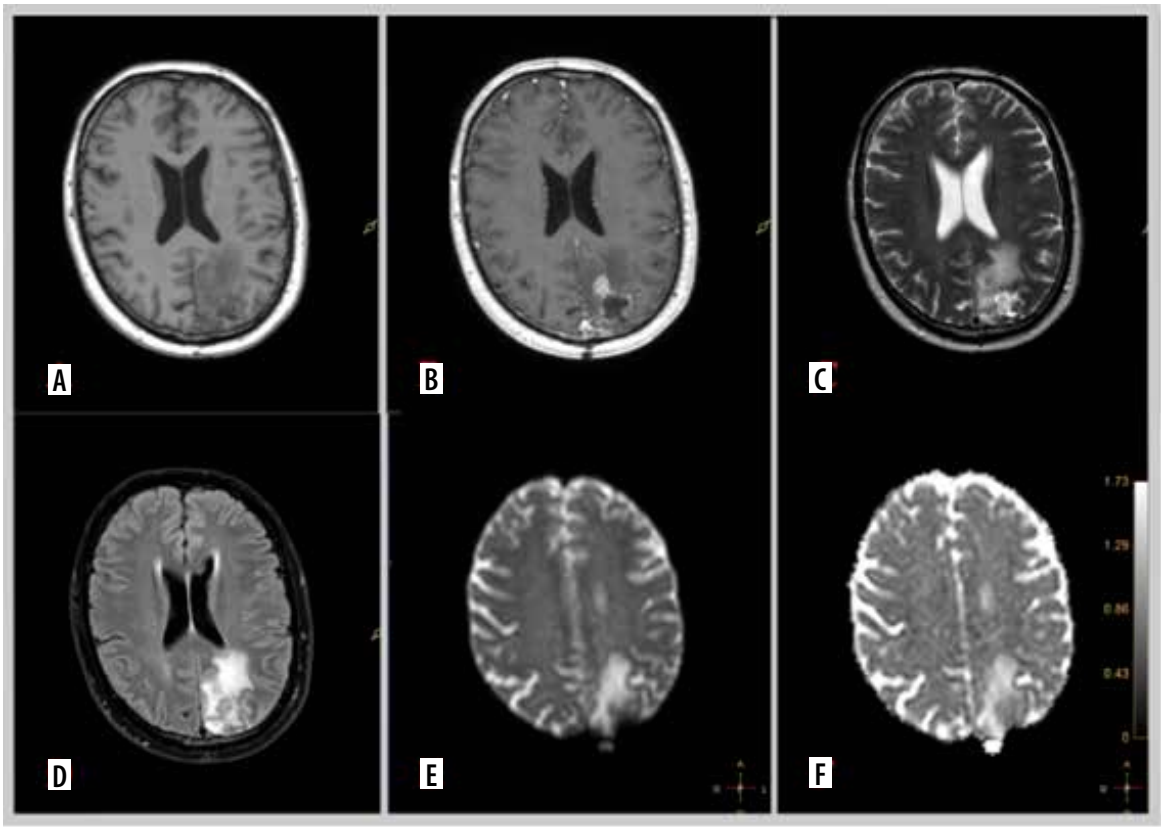

Figure 2. Representative magnetic resonance images of examined patient. A 67-year-old man with glioblastoma G4. Molecular characteristics: *IDH1*-wild-type, present *TERT* promoter pathogenic variant, *CDKN2A* homozygous deletion, *EGFR* amplification, *MGMT* promoter unmethylated. **A)** Pre-contrast T1. **B)** Contrast enhanced tumour on T1 post gadolinium. **C)** T2-weighted scan. **D)** Fluid-attenuated inversion recovery (FLAIR). **E**) Diffusion-weighted imaging (DWI). **F**) Apparent diffusion coefficient (ADC) map

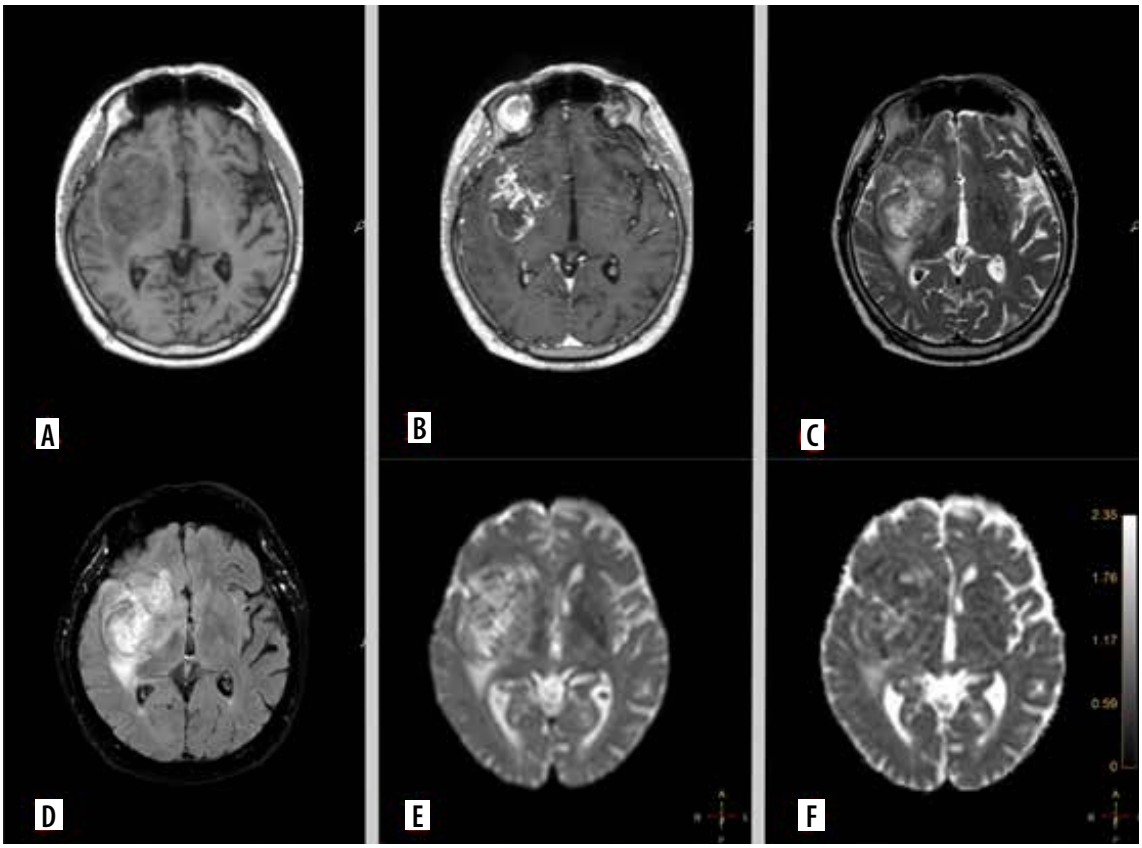

Figure 3. Representative magnetic resonance images of examined patient. A 52-year-old man with glioblastoma G4. Molecular characteristics: *IDH1*-wild-type, present *TERT* promoter pathogenic variant, *CDKN2A* non-deleted, *EGFR* non-amplification, *MGMT* promoter unmethylated. **A**) Pre-contrast T1. **B)** Contrast enhanced tumour on T1 post gadolinium. **C)** T2-weighted scan. **D)** Fluid-attenuated inversion recovery (FLAIR). **E)** Diffusion-weighted imaging (DWI).. **F)** ADC map

Table 3. Imaging parameters

	n	%
Contrast enhancement		
No	24	26.4
Yes	67	73.6
Enhancement quality		
0	24	26.4
1	12	13.2
2	55	62.6
T2/FLAIR mismatch		
No	82	90.1
Yes	9	9.9
rCBF (Mean; SD)	4.1	
rCBV (Mean; SD)	5.2	
Intratumoural necrosis		
No	25	27.5
Yes	66	72.5
Maximal diameter (mm) (mean; SD)	44.6	374.7
Volume (cm^3) (mean; SD)	31.12	429.5
Mean ADC ($\times 10^3$ mm^3s) (mean; SD)	1.36	

	n	%
Corpus callosum involvement		
No	66	72.5
Yes	25	27.5
Cortical involvement		
0	14	15.4
1	77	84.6
Ependymal extension		
0	32	35.2
1	59	64.8
Pial invasion		
No	23	25.3
Yes	68	74.7

rCBF – regional cerebral blood flow, rCBV – relative cerebral blood volume, ADC – apparent diffusion coefficient

Table 4. Relationship between magnetic resonance imaging perfusion and genetic features

		Mean ADC [x10-3mm²/s]		Contrast enhancement			Enhancement quality				T2/FLAIR mismatch			Intratumoural necrosis >5%			Corpus callosum involvement			Ependymal extension			Pial invasion			Cortical involvement		
		Mean	*p*	Absent	Present	*p*	0	1	2	*p*	Absent	Present	*p*	Absent	Present	*p*	Absent	Present	*p*	Absent	Present	*p*	Absent	Present	*p*	Absent	Present	*p*
IDH1 mutation	Wildtype	1.3	< 0.05	6	59	< 0.05	6	11	49	< 0.05	63	2	< 0.05	18	47		45	20		21	44		16	49		7	58	
	Mutant	1.52		18	8		18	1	7		19	7		7	19		21	5		11	15		7	19		7	19	
MGMT methylation	Unmethylated	1.21	< 0.05	3	30	< 0.05	3	3	27	< 0.05	31	2		11	22		27	6		13	20		7	26		4	29	
	Methylated	1.46		20	34		20	8	26		47	7		14	40		37	17		19	35		14	40		10	44	
EGFR amplification	No	1.47	< 0.05	17	23	< 0.05	17	3	20	< 0.05	34	6		12	28		33	7		17	23		8	32		9	31	
	Yes	1.26		6	41		6	8	33		45	2		13	34		32	15		15	32		12	35		5	42	
CDKN2A deletion	Non-deleted	1.51	< 0.05	17	24	< 0.05	17	3	21	< 0.05	37	4		9	32		35	6		19	22		12	29		9	32	
	Heterozygous deletion	1.21		3	25		3	3	22		26	2		11	17		21	7		8	20		4	24		3	25	
	Homozygous deletion	1.26		3	14		3	4	10		15	2		5	12		9	8		5	12		4	13		2	15	
TP53 deletion	No	1.36	< 0.05	23	55		23	9	46		70	8		23	55		59	19		30	48		19	59		12	66	
	Yes	1.95		0	3		0	0	3		3	0		0	3		3	0		0	3		0	3		1	2	
PDGFRA amplification	No	1.4		22	45		22	8	37		60	7		18	49		51	16		26	41		17	50		12	55	
	Yes	1.29		1	13		1	1	12		13	1		5	9		11	3		4	10		2	12		1	13	
PTEN deletion	No	1.42		21	24	< 0.05	21	1	23	< 0.05	38	7		10	35		37	8		20	25		6	39	< 0.05	11	34	< 0.05
	Yes	1.31		2	33		2	8	25		34	1		13	22		24	11		10	25		13	22		2	33	
1p19q codeletion	No	1.37		22	64		22	11	53		77	9		24	62		64	22		31	55		21	65		14	72	
	Yes	1.8		1	0		1	0	0		1	0		1	0		0	1		0	1		0	1		0	1	
TERT pathogenic variant	No	1.54	< 0.05	16	18	< 0.05	16	1	17	< 0.05	28	6		8	26		26	8		13	21		9	25		6	28	
	Yes	1.3		5	39		5	9	30		42	2		10	34		32	12		15	29		11	33		6	38	
H3k27 pathogenic variant	No	1.41		19	49		18	8	41		0	1		16	52		53	15		26	42		17	51		11	57	

Results are based on two-sided tests assuming equal variances.

IDH1 – isocitrate dehydrogenase 1, *MGMT* – O^6-methylguanine-DNA methyltransferase, *EGFR* – epidermal growth factor receptor, *CDKN2A* – loss of cyclin-dependent kinase inhibitor 2A, *PDGFRA* – platelet-derived growth factor receptor alpha gene, *PTEN* – phosphatase and tensin homologue, *TERT* – telomerase reverse transcriptase

with *MGMT* promoter methylation compared to unmethylated cases ($p < 0.05$). Similar trends were observed across other MRI parameters.

Gliomas without *EGFR* amplification had a higher mean ADC value compared to those with amplification ($p < 0.05$). Contrast enhancement was more common in *EGFR*-amplified gliomas compared to non-amplified cases ($p < 0.05$).

Gliomas with non-deleted *CDKN2A* exhibited a higher mean ADC value compared to heterozygous deletions and homozygous deletions ($p < 0.05$). Contrast enhancement was less frequent in gliomas with homozygous deletions compared to non-deleted gliomas ($p < 0.05$).

The mean ADC value was significantly higher in gliomas with *TP53* deletion compared to non-deleted *TP53* gliomas ($p < 0.05$).

Gliomas without *PDGFRA* amplification showed a higher mean ADC value compared to those with amplification, but this difference was not statistically significant.

Gliomas without *PTEN* deletion had a higher mean ADC value compared to those with *PTEN* deletion. This difference was statistically significant ($p < 0.05$). Contrast enhancement was more common in gliomas with *PTEN* deletion compared to non-deleted *PTEN* gliomas ($p < 0.05$).

Gliomas with *TERT* pathogenic variants exhibited a lower mean ADC value compared to those without the variant ($p < 0.05$). Contrast enhancement was more frequent in gliomas with *TERT* variants compared to those without ($p < 0.05$).

Discussion

The present study examines the significant relationship between DWI measures, particularly mean ADC values, and various genetic and molecular features of gliomas. The results of our research show that DWI and ADC values can be used as non-invasive indicators to predict genetic changes and tumour features. This is particularly significant in the setting of tumours where biopsy is challenging or unfeasible, providing a vital alternative for acquiring diagnostic and prognostic information without intrusive treatments.

IDH1 mutation status

Our results indicate that *IDH1*-wildtype gliomas exhibit significantly lower mean ADC values compared to *IDH1*-mutant gliomas. Mounting evidence suggests that mutations in the *IDH* gene family can decrease the production of α-ketoglutarate, resulting in the formation of the oncometabolite (R)-2-hydroxyglutarate. This, in turn, leads to an increase in cell proliferation or cellularity. Therefore, our findings align with previous studies suggesting that *IDH1* wildtype gliomas are typically more aggressive and have higher cellularity, resulting in lower ADC values [4,9-12]. The significant association between lower ADC values and the presence of contrast enhancement further supports the aggressive nature of *IDH1*-wildtype gliomas. Prompt determination of the *IDH1* gene status is crucial, particularly during the initial non-invasive diagnostic phase. The significance of the *IDH1* gene status determines the subsequent genetic tests necessary for a comprehensive diagnosis (layered report structure) and accurate classification of the tumour, as required by the current CNS5 classification [8].

MGMT methylation

The study reveals that gliomas with unmethylated promoter of *MGMT* have lower mean ADC values compared to methylated *MGMT* gliomas. This observation corroborates existing literature indicating that *MGMT* methylation is associated with better prognosis and lower cellular density, reflected in higher ADC values [5]. However, it is important to note that the relationship between ADC values and *MGMT* status has been strongly debated in the literature. Some studies, such as those by Romano *et al.* [13] and Moon *et al.* [14], report higher ADC values in methylated *MGMT* tumours, supporting the notion of lower cellular density in these tumours. Conversely, Pope *et al.* [15] and others have found lower ADC values in unmethylated tumours, suggesting that these results may not be consistent across all cases and may vary depending on the tumour region analysed (e.g. enhancing versus peritumoral tissue). The higher frequency of contrast enhancement in methylated *MGMT* gliomas suggest enhanced tumour permeability and angiogenesis, characteristics often observed in these tumours [16]. Early assessment of *MGMT* promoter methylation is vital for optimising treatment strategies and improving prognostication in glioma patients. Specifically, patients with methylated promoters respond better to temozolomide [17]. It also aids in risk stratification, guiding clinical decision-making, and enhancing clinical trial design by selecting appropriate patient cohorts [18]. Thus, integrating *MGMT* methylation assessment early in the diagnostic process is crucial for effective glioma patient management.

According to the recent CNS5 and cIMPACT-NOW, specific genetic alterations change the final diagnosis. Confirming the presence of certain genetic alterations in glioma can reclassify the tumour as "molecularly" high-grade, resulting in a considerably lower survival rate compared to gliomas without mutations [19]. *IDH1*-wildtype lower-grade gliomas that exhibit one of three particular genetic markers (*EGFR* amplification, +7/–10 abnormality, or *TERT* promoter alterations) are classified as the most malignant type of tumour, known as WHO grade 4 [20]. In *IDH1*-mutant lower-grade gliomas, the mutation of the highest malignancy is *CDKN2A* homozygous deletion. Hence, identifying these indicators during the initial phase of diagnosis potentially influences subsequent treat-

ment. Noninvasive assessment of molecular characteristics is primarily employed in patients for whom acquiring histopathology material is highly hazardous or unfeasible. For these patients, MRI and acquired ADC are advantageous because DWI is the typical sequence performed during initial diagnosis.

EGFR amplification

Gliomas without *EGFR* amplification showed higher mean ADC values compared to those with *EGFR* amplification. This is consistent with the notion that *EGFR* amplification is related to increased tumour aggressiveness and cellularity, resulting in lower ADC values [21]. The higher prevalence of contrast enhancement in *EGFR* amplified gliomas further underscores their aggressive phenotype.

CDKN2A deletion

In the presented study non-deleted *CDKN2A* gliomas exhibited higher mean ADC values compared to those with heterozygous or homozygous deletions. *CDKN2A* deletions are known to contribute to tumour progression and malignancy, which could be reflected in lower ADC values [22]. The relationship between *CDKN2A* gene status and ADC value has been investigated in several studies, which have shown contradictory findings. Indeed, certain research has shown a substantial correlation between ADC and *CDKN2A*, although in other studies the correlation is not statistically significant [23,24].

TERT pathogenic variants

TERT is an enzyme responsible for maintaining telomeres that safeguard genomic integrity during cell division. *TERT* is highly expressed in stem cells and cancer cells, playing a crucial role in cellular immortality. Mutations in promoter of *TERT* are a hallmark of various cancers, including glioblastoma, and they are commonly used as diagnostic and prognostic markers. Suppression of *TERT* by promotion mutation expression has been shown to increase cellular sensitivity to DNA damage, making *TERT* a promising target for novel therapeutic approaches in GBM. In our study, gliomas with *TERT* pathogenic variants exhibited lower mean ADC values, indicative of higher tumour cellularity and increased aggressiveness, which is in line with previous research [25]. This finding aligns with the established role of *TERT* mutations in promoting tumour proliferation and malignancy. Additionally, the significant association between *TERT* promoter mutations and increased contrast enhancement on MRI further underscores the aggressive nature of these tumours. Contrast enhancement reflects the disruption of the blood-brain barrier and neovascularisation, which are characteristic of high-grade, rapidly growing tumours. The combined observation of lower ADC values and greater contrast enhancement in *TERT*-mutant gliomas provides robust non-invasive indicators of tumour aggressiveness and highlights the potential utility of advanced imaging techniques in the characterisation and management of these malignancies.

In summary, this study highlights the utility of DWI and ADC values in non-invasively predicting the genetic and molecular landscape of gliomas. The significant correlations between imaging biomarkers and genetic features underscore the potential of advanced MRI techniques in guiding personalised treatment approaches.

Limitations of the study

Despite the promising findings and significant insights provided by this study, several limitations should be acknowledged to contextualise the results and guide future research.

Firstly, the study cohort, although comprehensive, was relatively small and drawn from a single institution. This limits the generalisability of the findings across broader populations and different clinical settings. Larger, multicentre studies are necessary to validate these results and account for potential variations in imaging protocols, genetic testing methods, and patient demographics. Secondly, the study's retrospective design inherently introduces certain biases, including selection bias and information bias. The study also relied heavily on mean ADC values, which, while informative, may not capture the full complexity of tumour diffusion characteristics. ADC values can be influenced by various factors, including tumour heterogeneity, necrosis, and surrounding oedema. Advanced diffusion imaging techniques, such as diffusion tensor imaging (DTI) and diffusion kurtosis imaging (DKI), might provide more detailed insights into the microstructural properties of gliomas.

Future directions

This study reveals the potential of DWI and ADC values in glioma characterisation and treatment planning. To validate these associations, larger, multicentre cohorts are needed to account for variations in imaging protocols, genetic testing methods, and patient demographics. Longitudinal studies tracking changes in ADC values during and after treatment can provide insights into tumour response and resistance mechanisms. Moreover, further research is needed to understand the biological mechanisms driving the observed correlations between ADC values and genetic alterations. Automated analysis tools leveraging artificial intelligence and machine learning can facilitate the processing of large imaging datasets and aid in real-time clinical decision-making. Expanding research to include paediatric populations and rare glioma subtypes will ensure the benefits of advanced imaging techniques are realised across diverse patient groups.

Conclusions

This study underscores the significant potential of DWI and mean ADC values as non-invasive biomarkers for predicting genetic and molecular characteristics of gliomas. Our findings demonstrate that lower ADC values are generally associated with more aggressive tumour phenotypes and specific genetic alterations, such as *IDH1*-wildtype, *MGMT* unmethylated status, *EGFR* amplification, and *CDKN2A* homozygous deletion.

In conclusion, DWI and ADC metrics provide critical insights into the genetic and molecular landscape of gliomas, offering a non-invasive and effective tool for enhancing diagnostic precision and tailoring therapeutic interventions. This study highlights the transformative potential of advanced imaging in the era of personalised oncology, ultimately aiming to improve patient outcomes through more targeted and informed treatment strategies.

Disclosures

1. Institutional review board statement: The study was conducted in accordance with the Declaration of Helsinki, and the Ethics Committee of the Nicolaus Copernicus University, Collegium Medicum in Bydgoszcz, Poland approved the study protocol.
2. Assistance with the article: None.
3. Financial support and sponsorship: None.
4. Conflicts of interest: None.

References

1. Weller M, Wick W, Aldape K, Brada M, Berger M, Pfister SM, et al. Glioma. Nat Rev Dis Primer 2015; 1: 15017. DOI: https://doi.org/10.1038/nrdp.2015.17.
2. Hagmann P, Jonasson L, Maeder P, Thiran JP, Wedeen VJ, Meuli R. Understanding diffusion MR imaging techniques: from scalar diffusion-weighted imaging to diffusion tensor imaging and beyond. Radiogr Rev Publ Radiol Soc N Am Inc 2006; 26 Suppl 1: S205-S223. DOI: https://doi.org/10.1148/rg.26si065510.
3. Zhang L, Min Z, Tang M, Chen S, Lei X, Zhang X. The utility of diffusion MRI with quantitative ADC measurements for differentiating high-grade from low-grade cerebral gliomas: evidence from a meta-analysis. J Neurol Sci 2017; 373: 9-15.
4. Xing Z, Yang X, She D, Lin Y, Zhang Y, Cao D. Noninvasive assessment of IDH mutational status in World Health Organization grade II and III astrocytomas using DWI and DSC-PWI combined with conventional MR imaging. Am J Neuroradiol 2017; 38: 1138-1144.
5. Śledzińska P, Bebyn MG, Furtak J, Kowalewski J, Lewandowska MA. Prognostic and predictive biomarkers in gliomas. Int J Mol Sci 2021; 22: 10373. DOI: https://doi.org/10.3390/ijms221910373.
6. Śledzińska P, Bebyn M, Szczerba E, Furtak J, Harat M, Olszewska N, et al. Glioma 2021 WHO classification: the superiority of NGS over IHC in routine diagnostics. Mol Diagn Ther 2022; 26: 699-713.
7. VASARI Research Project – The Cancer Imaging Archive (TCIA) Public Access – Cancer Imaging Archive Wiki n.d. Available at: https://wiki.cancerimagingarchive.net/display/Public/VASARI+Research+Project (Accessed: 10.08.2024).
8. Louis DN, Perry A, Wesseling P, Brat DJ, Cree IA, Figarella-Branger D, et al. The 2021 WHO classification of tumors of the central nervous system: a summary. Neuro Oncol 2021; 23: 1231-1251.
9. Leu K, Ott GA, Lai A, Nghiemphu PL, Pope WB, Yong WH, et al. Perfusion and diffusion MRI signatures in histologic and genetic subtypes of WHO grade II-III diffuse gliomas. J Neurooncol 2017; 134: 177-188.
10. Thust SC, Hassanein S, Bisdas S, Rees JH, Hyare H, Maynard JA, et al. Apparent diffusion coefficient for molecular subtyping of non-gadolinium-enhancing WHO grade II/III glioma: volumetric segmentation versus two-dimensional region of interest analysis. Eur Radiol 2018; 28: 3779-3788.
11. Maynard J, Okuchi S, Wastling S, Busaidi AA, Almossawi O, Mbatha W, et al. World Health Organization grade II/III glioma molecular status: prediction by MRI morphologic features and apparent diffusion coefficient. Radiology 2020; 296: 111-121.
12. Kim M, Jung SY, Park JE, Jo Y, Park SY, Nam SJ, et al. Diffusion- and perfusion-weighted MRI radiomics model may predict isocitrate dehydrogenase (IDH) mutation and tumor aggressiveness in diffuse lower grade glioma. Eur Radiol 2020; 30: 2142-2151.
13. Romano A, Calabria LF, Tavanti F, Minniti G, Rossi-Espagnet MC, Coppola V, et al. Apparent diffusion coefficient obtained by magnetic resonance imaging as a prognostic marker in glioblastomas: correlation with MGMT promoter methylation status. Eur Radiol 2013; 23: 513-520.
14. Moon WJ, Choi JW, Roh HG, Lim SD, Koh YC. Imaging parameters of high grade gliomas in relation to the MGMT promoter methylation status: the CT, diffusion tensor imaging, and perfusion MR imaging. Neuroradiology 2012; 54: 555-563.
15. Pope WB, Lai A, Mehta R, Kim HJ, Qiao J, Young JR, et al. Apparent diffusion coefficient histogram analysis stratifies progression-free survival in newly diagnosed bevacizumab-treated glioblastoma. AJNR Am J Neuroradiol 2011; 32: 882-889.
16. Ellingson BM. Radiogenomics and imaging phenotypes in glioblastoma: novel observations and correlation with molecular characteristics. Curr Neurol Neurosci Rep 2015; 15: 506. DOI: https://doi.org/10.1007/s11910-014-0506-0.
17. Hegi ME, Diserens AC, Gorlia T, Hamou MF, de Tribolet N, Weller M, et al. MGMT gene silencing and benefit from temozolomide in glioblastoma. N Engl J Med 2005; 352: 997-1003.
18. Weller M, Stupp R, Reifenberger G, Brandes AA, van den Bent MJ, Wick W, et al. MGMT promoter methylation in malignant gliomas: ready for personalized medicine? Nat Rev Neurol 2010; 6: 39-51.
19. Aibaidula A, Chan AKY, Shi Z, Li Y, Zhang R, Yang R, et al. Adult IDH wild-type lower-grade gliomas should be further stratified. Neuro Oncol 2017; 19: 1327-1337.

20. Brat DJ, Aldape K, Colman H, Holland EC, Louis DN, Jenkins RB, et al. cIMPACT-NOW update 3: recommended diagnostic criteria for "Diffuse astrocytic glioma, IDH-wildtype, with molecular features of glioblastoma, WHO grade IV." Acta Neuropathol (Berl) 2018; 136: 805-810.
21. Park YW, Park JE, Ahn SS, Kim EH, Kang SG, Chang JH, et al. Magnetic resonance imaging parameters for noninvasive prediction of epidermal growth factor receptor amplification in isocitrate dehydrogenase-wild-type lower-grade gliomas: a multicenter study. Neurosurgery 2021; 89: 257-265.
22. Appay R, Dehais C, Maurage CA, Alentorn A, Carpentier C, Colin C, et al. CDKN2A homozygous deletion is a strong adverse prognosis factor in diffuse malignant IDH-mutant gliomas. Neuro Oncol 2019; 21: 1519-1528.
23. Park YW, Park KS, Park JE, Ahn SS, Park I, Kim HS, et al. Qualitative and quantitative magnetic resonance imaging phenotypes may predict CDKN2A/B homozygous deletion status in isocitrate dehydrogenase-mutant astrocytomas: a multicenter study. Korean J Radiol 2023; 24: 133-144.
24. Chiang GC, Pisapia DJ, Liechty B, Magge R, Ramakrishna R, Knisely J, et al. The prognostic value of MRI subventricular zone involvement and tumor genetics in lower grade gliomas. J Neuroimaging 2020; 30: 901-909.
25. Chen L, Chen R, Li T, Huang L, Tang C, Li Y, et al. MRI radiomics model for predicting TERT promoter mutation status in glioblastoma. Brain Behav 2023; 13: e3324. DOI: https://doi.org/10.1002/brb3.3324.